Organic & Biomolecular Chemistry

rsc.li/obc

ROYAL SOCIETY
OF **CHEMISTRY**
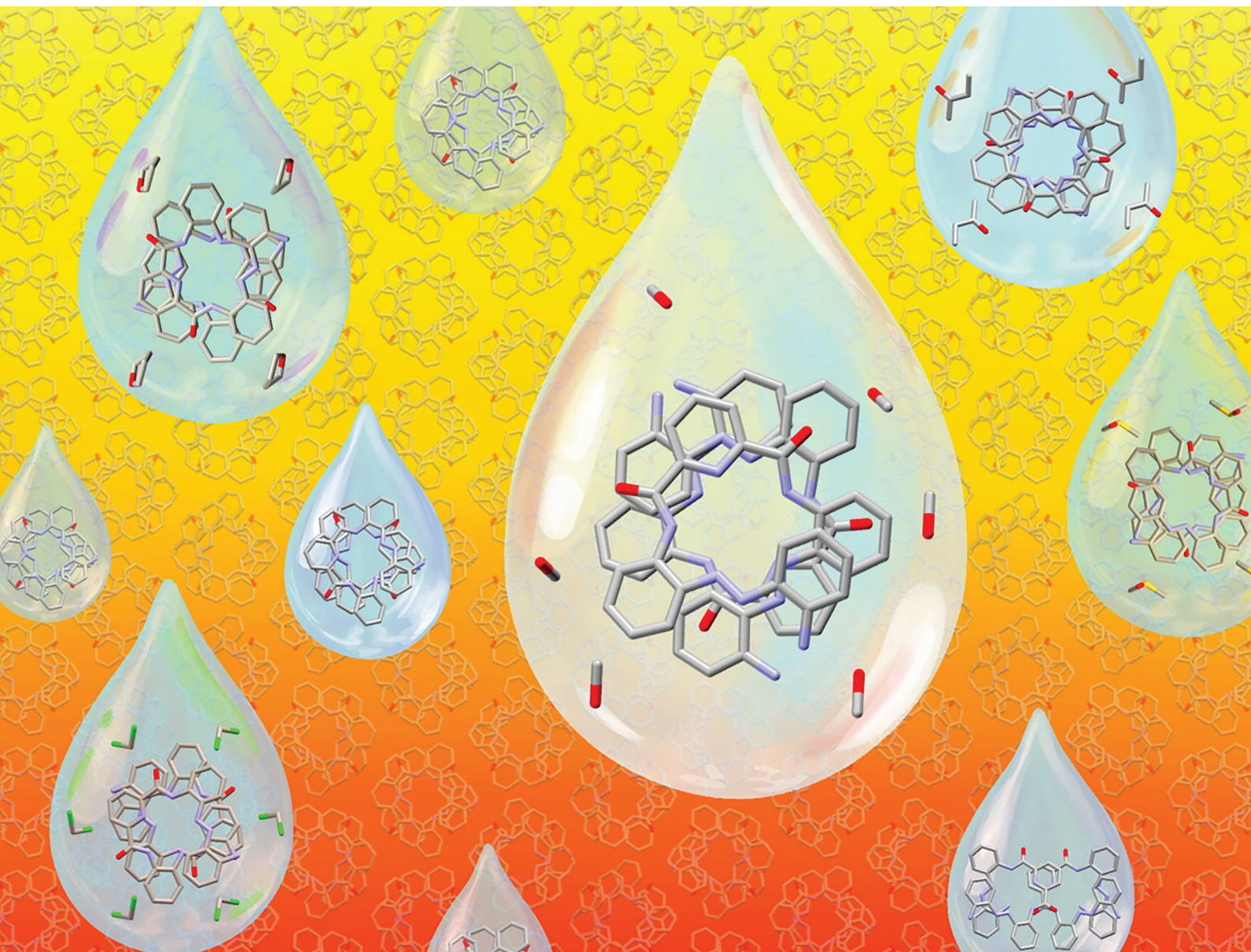
PAPER
Sarah J. Pike *et al.*
Solvatomorphism of a 2,6-pyridyldicarboxamide-based
foldamer

Solvatomorphism of a 2,6-pyridyldicarboxamide-based foldamer†

Sena Ozturk,[a] Alexander R. Davis,[a] Colin C. Seaton, [b] Louise Male [a] and Sarah J. Pike [*a]

A detailed solvatomorphism study conducted on a diamine-terminated 2,6-pyridyldicarboxamide-based foldamer **1** is reported. This investigation establishes the influence of a diverse range of polar and non-polar solvents including chloroform (**1A**), a trifluorotoluene/dichloromethane mixture (**1A**), dimethyl-formamide/diethyl ether (**1B**), tetrahydrofuran (**1**·THF), butanone (**1**·butanone), dichloromethane (**1**·DCM), a methanol/dichloromethane mixture (**1**·MeOH) and dimethylsulfoxide (**1**·DMSO) on the solid-state conformation and crystal packing behaviour of this supramolecular scaffold. Single-crystal X-ray diffraction analysis of the seven solvatomorphs of the studied foldamer (**1A**, **1B**, **1**·DCM, **1**·THF, **1**·butanone, **1**·MeOH and **1**·DMSO) identified that **1**·DCM, **1**·THF, **1**·butanone, **1**·MeOH and **1**·DMSO form supramolecular aggregates (*e.g.*, channels/cavities) which incorporate solvent molecules within the voids of the system, leading them to adopt channels of differing dimensions between 3.5 and 9.0 Å. Solid-state analysis identified that a diverse array of intermolecular non-covalent interactions form between the foldamer and the solvent molecule, including N–H···O, N–H···Cl, O–H···O, N–H···Cl and C–H···O hydrogen-bonding interactions, stabilising the formation of these solvent-mediated channel aggregates within the different solvatomorphs of the studied foldamer. We envisage that these solvatomorphism studies will facilitate the future design of foldamers, particularly given the emerging solid-state applications of foldamers which could hold relevance in the field of crystal engineering or for the uptake of small molecules for long-term use in energy storage and materials chemistry.

Introduction

Foldamers are synthetic oligomers that adopt stable conformations inspired by those found in natural systems (*e.g.*, helices).[1–3] Foldamers have garnered much attention due to their widespread applications in a diverse range of areas including synthesis as catalysts,[4,5] supramolecular chemistry as sensors and probes[6–8] and biological chemistry due to their potent anti-cancer, anti-fungal and anti-bacterial activities.[9,10] Moreover, in recent years, foldamers have found an increasing number of applications in the solid state, including crystal engineering[11] and materials science,[12,13] for example, with reports of their molecular transport properties.[14]

Solvatomorphism refers to the ability of a compound to exist in different solid-state forms. Solvatomorphs exhibit a number of crystalline states wherein their unit cells show distinct elemental compositions due to the incorporation of one or more solvent molecules.[15] The propensity of different solvatomorphs of a compound to exhibit distinct physical properties (*e.g.*, stability, bioavailability and solubility) can affect their activity.[15] Consequently, this has led to them attracting great interest, particularly in pharmaceuticals,[15] and more recently, in supramolecular chemistry.[16–18]

The role of solvent in controlling the behaviour of foldamers has been studied for a range of foldamer classes including aromatic oligoamides,[19,20] *m*PE[21] and aminoisobutyric acid foldamers.[22] However, many of these solvent-based studies conducted on foldamers focus on their behaviour in solution. Conversely, solid-state studies undertaken on foldamers are generally conducted to elucidate the nature of the intramolecular non-covalent interactions that govern the conformational behaviour[23–25] and self-assembly[26] of these supramolecular scaffolds without extensively exploring solvent effects in the solid state. The influence of solvent on the self-assembly of foldamers has been used to control the formation of vesicles and organogels.[27] Solvent effects have also been

*a*School of Chemistry, University of Birmingham, Edgbaston, Birmingham, B15 2TT, UK. E-mail: s.j.pike@bham.ac.uk
*b*School of Chemistry and Biosciences, Faculty of Life Sciences, University of Bradford, Bradford, West Yorkshire, BD7 1DP, UK

used to control the adoption of topologically distinct structures within foldamers including regulating the interplay between linear structures and dimers[28] and controlling the preference for dimerization between helices with opposite or identical handedness in stable head-to-tail dimers in different chlorinated solvents.[29] Solvent effects can also play an important role in the formation of solvent channels and pores in the solid state in a diverse array of structures including metal–organic frameworks,[30] carbon–organic frameworks,[31] proteins[32] and other materials.[33] However, despite the importance of crystallographic studies into the solvatomorphism of foldamers, studies which systematically consider the role of solvent in the solid state are limited.[34,35] This lack of data leaves this important area largely unexplored for these supramolecular scaffolds which, in turn, restricts the development of the field.

In 2016, Nissinen and co-workers highlighted the importance of solvatomorphism in controlling the conformational behaviour of foldamers, when they used single-crystal X-ray diffraction analysis to assess the influence of a range of solvents including polar protic (*e.g.*, methanol and ethanol), polar non-protic (*e.g.*, dimethylsulfoxide, tetrahydrofuran, dioxane, acetonitrile, dimethylacetamide, and ethyl acetate) and non-polar aprotic solvents (*e.g.*, toluene) on the solid-state behaviour of a series of aromatic oligoamide foldamers.[36] In this solvatomorphism study, it was identified that two general conformations of a protohelical @-conformation and a sigmoidal *S*-conformation were adopted for the studied aromatic oligoamide foldamers. In the protohelical @-conformation, the packing coefficients were generally slightly larger than in the sigmoidal *S*-conformation as it was established that the @-conformation lacked void spaces. Conversely, the sigmoidal *S*-conformation for these scaffolds exhibits a less compact crystal packing arrangement wherein for a selection of the studied aromatic oligoamide foldamers, solvent molecules (*e.g.*, dimethylacetamide) occupy the void spaces within the structure.[37] However, despite these reports and the growing solid-state applications of foldamers (*e.g.*, in crystal engineering and materials science), studies into the solvatomorphism of these supramolecular scaffolds remain rare, and this lack of information limits the progression of the field.

Herein, we report on a solvatomorphism study of a diamine terminated 2,6-pyridyldicarboxamide-based foldamer **1** (see Fig. 1).[38] The incorporation of amine functionalities at the termini of the foldamer offers the opportunity for these supramolecular scaffolds to interact with a diverse range of solvents (*e.g.*, by forming hydrogen bonds with an appropriate solvent molecule). This detailed investigation of seven solvatomorphs of **1A**, **1B**, **1·DCM**, **1·THF**, **1·butanone**, **1·MeOH** and **1·DMSO** identifies the influence of solvent on governing the conformational preferences and crystal packing arrangements of these supramolecular scaffolds. Furthermore, crystallographic analysis has identified the presence of a range of supramolecular aggregates in these solvatomorphs including channels and one-dimensional hydrogen-bonding chains. In-depth solid-state analysis has also established that the dimensions of the supramolecular channel aggregates within the solvatomorphs of the studied foldamer vary significantly (between 3.5 and 9.0 Å) as a function of the solvent used under the crystallisation conditions.

Results and discussion

Synthesis and crystallographic conditions for foldamer 1

The amine-terminated foldamer **1** was synthesised using a linear five-step procedure in accordance with known literature procedures (see the ESI†).[39,40] To determine the influence of solvent on the solid-state behaviour of **1**, single crystals suitable for X-ray diffraction analysis were grown in a diverse array of solvents including chloroform, trifluorotoluene/dichloromethane, dimethylformamide, butanone, tetrahydrofuran, dichloromethane, methanol and dimethylsulfoxide. From this solvent screening, seven distinct solvatomorphs of the foldamer including **1A** (from chloroform and trifluorotoluene/dichloromethane respectively), **1B** (from dimethylformamide), **1·DCM** (from dichloromethane), **1·THF** (from tetrahydrofuran), **1·butanone** (from butanone), **1·MeOH** (from methanol) and **1·DMSO** (from dimethylsulfoxide) were successfully accessed. Unfortunately, the additional tested solvents of acetone, ethanol, pyridine, 1,4-dioxane, dimethylformamide/diethyl ether, ethyl acetate, toluene, xylene, 2-decanone, 2-hexanone, 3-hexanone and 2-ethoxyethanol did not lead to crystals of sufficiently good quality for single-crystal X-ray diffraction analysis (see the ESI† for further details).

Crystallographic analysis of foldamer solvatomorphs

Crystallographic analysis carried out on **1A**, **1B**, **1·DCM**, **1·THF**, **1·butanone**, **1·MeOH** and **1·DMSO** allowed for the determination of the conformational preferences of the scaffolds in the solid state (*i.e.*, the presence of a stable helical conformation) and the quantification of the helical pitch values of the foldamer scaffolds.[41] Furthermore, solid-state analysis of these solvatomorphs has established the presence or absence of supramolecular aggregates, including channels/cavities and one-dimensional hydrogen-bonded chains, in the solid state.
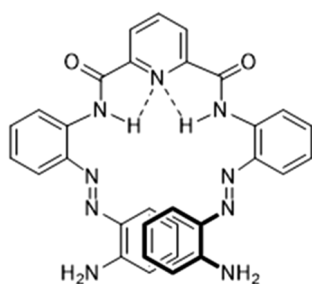

Fig. 1 Structure of the amine-terminated 2,6-pyridyldicarboxamide foldamer **1** whose solvatomorphism is investigated in this work using single-crystal X-ray diffraction analysis.

This journal is © The Royal Society of Chemistry 2025

Org. Biomol. Chem., 2025, **23**, 5590–5599 | **5591**

The influence of the solvent used under the crystallisation conditions on the nature and size of the supramolecular channel aggregates formed in the solid state has been determined through quantification of the channel cavity dimensions.[42] Additionally, X-ray crystallographic analysis has identified the presence of a range of intramolecular and intermolecular non-covalent interactions including π–π stacking and the presence of N–H⋯O, N–H⋯Cl, O–H⋯O and C–H⋯O hydrogen-bonding interactions[43] that support the crystal packing arrangements observed in these structures. Selected crystallographic data and details for **1A**, **1B**, **1·DCM**, **1·THF**, **1·butanone**, **1·MeOH** and **1·DMSO**, including crystallisation solvent, compound name, whether the solvatomorph is a racemate or a conglomerate, and the crystal packing arrangement, are presented in Table 1.

General similarities in the solid-state behaviour of the foldamer solvatomorphs

In all of the crystal structures obtained for the foldamer (*i.e.*, **1A**, **1B**, **1·DCM**, **1·THF**, **1·butanone**, **1·MeOH** and **1·DMSO**), the scaffold adopts a helical conformation that is stabilised by the presence of hydrogen-bonding interactions formed between the N atom of the central pyridyl unit and the NH atoms of the adjacent amide bonds (see Fig. 2a and the ESI†).[44] This intramolecular hydrogen-bonding motif enables the adoption of a *syn–syn* conformation that introduces curvature into the scaffold.[45] Additionally, the incorporation of the azobenzene units, both of which adopt *E*-geometry, on either side of the central pyridyl unit further extends the helical conformation of **1** in all the studied foldamers (see Fig. 2a and the ESI†).[46]

For all the studied structures of **1A**, **1B**, **1·DCM**, **1·THF**, **1·butanone**, **1·MeOH** and **1·DMSO**, comparable dimensions for the central 2,6-pyridyldicarboxamide cavity are observed
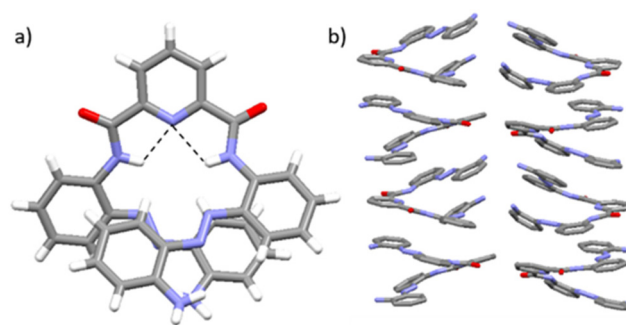

Fig. 2 X-ray structure of **1**: (a) viewed from above showing the adoption of a helical conformation in the solid state stabilised by the presence of the intramolecular hydrogen-bonding interactions between the NH groups of the carboxamide units and the N atom of the central pyridine; (b) viewed side-on showing the presence of the columnar crystal packing arrangement composed of stacks of helical molecules of alternating screw-sense preferences. C atoms are shown in grey, O in red, N in light blue and H in white. H-bonding interactions are shown as dashed red lines. H atoms have been removed from (b) for clarity.

(see the ESI†). As a consequence of the restricted size and shape of the central 2,6-pyridyldicarboxamide cavities in the studied foldamers, no solvent molecules are encapsulated into this central 2,6-pyridyldicarboxamide cavity under the studied crystallisation conditions (see Fig. 2 and the ESI†). Presumably, the encapsulation of solvent molecules within this central 2,6-pyridyldicarboxamide cavity of the foldamer is not favourable as it could disrupt the intramolecular hydrogen-bonding N–H⋯N⋯H–N motif that stabilises the *syn–syn* conformation of the scaffold. Further inspection of the crystal packing behaviour of **1A**, **1B**, **1·DCM**, **1·THF**, **1·butanone**, **1·MeOH** and **1·DMSO** shows that for all the studied systems, the same columnar packing arrangement composed of stacks of foldamer molecules is observed (see Fig. 2b and the ESI†). This crystal packing arrangement is supported by a range of intermolecular non-covalent interactions including intermolecular offset, face-to-face π–π stacking interactions,[43] and intermolecular N–H⋯O, N–H⋯Cl, O–H⋯O and C–H⋯O hydrogen-bonding interactions (see the ESI†).[43]

Detailed solid-state analysis of the foldamer solvatomorphs

Crystallographic analysis of 1. Two of the tested crystallisation conditions of slow evaporation of saturated solutions of the foldamer in (i) chloroform and (ii) a trifluorotoluene/dichloromethane solvent mixture gave the same crystallographic species: **1A** (see Table 1). In the unit cell of **1A**, there are two distinct foldamer molecules present and the presence of molecules with both *M*- and *P*-helicity shows that **1A** exists as a racemate in the solid state. There are no solvent molecules present in **1A** (see Fig. 3). The slow evaporation of a saturated dimethylformamide solution of the foldamer generated crystals of **1B**, which similarly show two distinct foldamers (*M*- and *P*-helicity) in the unit cell and no solvent (see the ESI†). These distinct foldamer molecules in the unit cells of **1A** and **1B** exhibit different helical pitches of 3.2, 3.5, 3.9 and 4.3 Å

Table 1 Summary of crystal data for single crystals of **1** grown under different crystallization conditions[a]

Crystallisation Solvent	Compound	Racemate/ conglomerate	Packing arrangement[b]
Chloroform	**1A**	Racemate	No channel
Trifluorotoluene/ dichloromethane	**1A**	Racemate	No channel
Dimethylformamide/ diethyl ether	**1B**	Racemate	No channel
Tetrahydrofuran	**1·THF**	Conglomerate	7.8 Å channel
Butanone	**1·butanone**	Conglomerate	9.0 Å channel[c]
Dichloromethane	**1·DCM**	Racemate	4.3 Å channel[d]
Methanol	**1·MeOH**	Racemate	3.5 Å channel[d]
Dimethylsulfoxide	**1·DMSO**	Conglomerate	8.7 Å channel[c]

[a] The following abbreviations have been used; DCM = dichloromethane, DMSO = dimethylsulfoxide, MeOH = methanol and THF = tetrahydrofuran. [b] MoloVol[42] was used for crystallographic analysis of the solid state structures and to quantify the dimensions of the supramolecular aggregates (*e.g.*, channels). [c] Disorder within the crystal structure led to two different channel dimensions being calculated, so an average of the structures was determined. [d] Diameters of the cavities were estimated using the van der Waals radii of atoms surrounding the depicted structure to calculate the distance as a cross section through the cavity in Olex2.
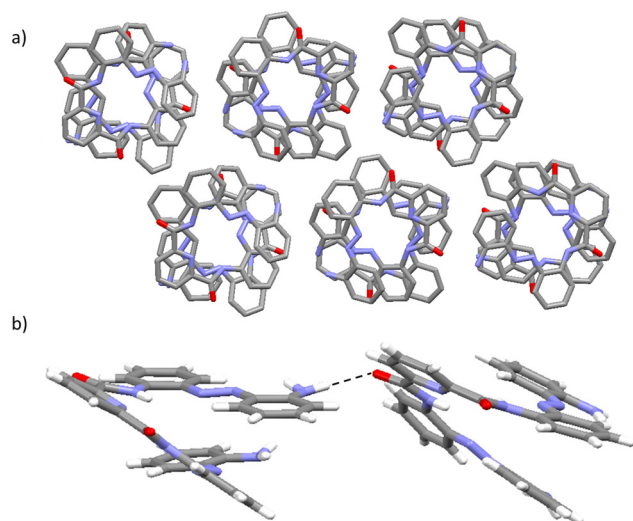
5592 | *Org. Biomol. Chem.*, 2025, **23**, 5590–5599

This journal is © The Royal Society of Chemistry 2025

Fig. 3 X-ray structure of **1A**: (a) viewed along the *a*-axis highlighting the presence of supramolecular aggregates in the form of channels within the void spaces in the solid state; (b) highlighting the presence of an intermolecular N−H⋯O hydrogen-bonding interaction between foldamer molecules of opposite handedness in adjacent columnar stacks. C atoms are shown in grey, O in red, N in light blue and H in white. H-bonding interactions are shown as dashed red lines. H atoms have been removed from (a) for clarity.

(see the ESI†).[41] The observed variation in the helical pitch is likely a consequence of the differing relative orientations of the terminal amine groups in the foldamer molecules in **1A** and **1B** with respect to the rest of the foldamer scaffold. Notably, some of the terminal amine groups in **1A** and **1B** lie within the same plane as the aromatic ring of the terminal aniline group of the foldamer whilst others reside outside of the plane of the terminal aromatic functionality (see the ESI†). These differing orientations of the amine groups observed in **1A** and **1B** are likely a result of subtle crystal packing forces, for example, through the ability of some of the NH groups of the terminal amine functionality to form intermolecular N−H⋯O hydrogen-bonding interactions[44] with adjacent foldamer molecules (Fig. 3b and the ESI†). The presence of differing non-covalent interactions involving the NH amine protons for the distinct molecules in **1A** and **1B** is likely to have a significant influence on the helical pitch exhibited by the scaffold as the helical pitch is measured as the distance between the N atoms in the terminal amine functionalities in these systems.[41] In these solvent-free structures of **1A** and **1B**, there are no channels present in the solid state due to a high packing density in these solvatomorphs (see Table 1 and the ESI†).

Crystallographic analysis of 1·THF. Single crystals of **1·THF** suitable for X-ray diffraction analysis were grown through the slow vapour diffusion of diethyl ether into a saturated THF solution of **1** (see Fig. 4). In **1·THF**, there is one foldamer molecule and one THF solvent molecule present within the unit cell. The THF solvent molecule in **1·THF** is disordered across all atoms. **1·THF** forms a conglomerate wherein the foldamer
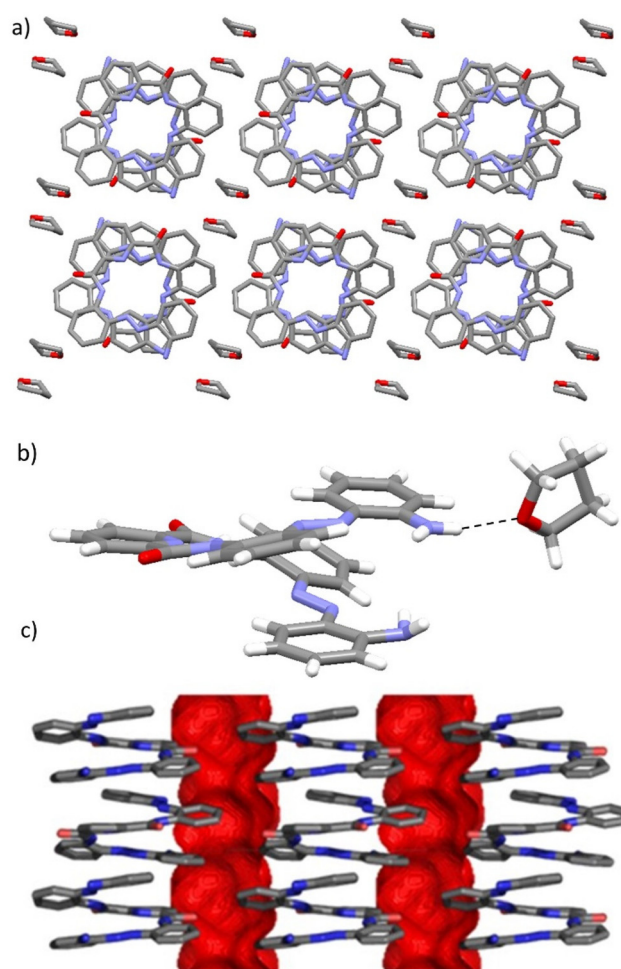

Fig. 4 X-ray structure of **1·THF**: (a) viewed along the *b*-axis highlighting the presence of the tetrahydrofuran solvent molecules within the void spaces of the crystal packing arrangement of the structure; (b) showing the presence of intermolecular N−H⋯O and hydrogen-bonding interactions formed between the foldamer and a tetrahydrofuran solvent molecule which help stabilise the incorporation of tetrahydrofuran solvent molecules into the channel cavities within the structure; (c) showing the calculation of the channel cavity dimensions using MoloVol.[42] C atoms are shown in grey, O in red, N in light blue and H in white. H-bonding interactions are shown as dashed red lines. H atoms have been removed from (a) for clarity. The disorder about the THF solvent molecules has been removed for clarity.

molecules observed in the solid state adopt one type of helical handedness (*P*-helicity) (see Table 1).[47] Such crystalline behaviour is unusual for achiral foldamers but has been previously observed for other 2,6-pyridyldicarboxamide-based foldamers[38a] as well as those in other foldamer classes.[48] The foldamer molecules in **1·THF** exhibit a helical pitch value of 3.4 Å which indicates the presence of a tight folded conformation (see the ESI†).

In the crystal packing arrangement of **1·THF**, columnar stacks composed of molecules of only *P*-helicity are observed. Hence, the crystal packing of **1·THF** differs from that observed in **1A** and **1B** which exhibit a columnar arrangement composed of alternating molecules of opposite helical handedness

This journal is © The Royal Society of Chemistry 2025

Org. Biomol. Chem., 2025, **23**, 5590–5599 | **5593**

within the same stack due to the differing adoption of conglomerates (in **1**·THF) and racemates (in **1A** and **1B**). Within the crystal packing arrangement of **1**·THF, the presence of channels is observed wherein disordered THF molecules reside within the void spaces of these supramolecular aggregates. Due to the disorder about the THF solvent molecules, it is not possible to comment on their relative arrangement within the channel's cavity (see the ESI†). The channels in **1**·THF exhibit a diameter of 7.8 Å (see Table 1 and Fig. 4c). The encapsulation of the THF molecules within the void spaces of the channels in **1**·THF is stabilised by the formation of intermolecular hydrogen-bonding interactions between the foldamer and solvent molecules. Specifically, there is an intermolecular N–H⋯O hydrogen-bonding interaction[44] between the NH atom of one of the terminal amine functionalities and the O atom of the THF solvent molecule (see Fig. 4b).

Crystallographic analysis of 1·butanone. Single crystals of **1**·butanone were grown through the slow evaporation of **1** in a saturated solution of butanone (see Fig. 5). In the unit cell of **1**·butanone, there is one foldamer molecule and one butanone molecule present. As observed in **1**·THF, solid-state analysis of

Fig. 5 X-ray structure of **1**·butanone: (a) viewed along the *b*-axis highlighting the presence of the butanone solvent molecules occupying spaces within the channel crystal packing arrangement of the structure; (b) showing the presence of intermolecular N–H⋯O and hydrogen-bonding interactions formed between the foldamer and a butanone solvent molecule which help stabilise the incorporation of butanone solvent molecules into the channel cavities within the structure. C atoms are shown in grey, O in red, N in light blue and H in white. H-bonding interactions are shown as dashed red lines. H atoms have been removed from (a) for clarity.

1·butanone shows that this solvatomorph forms a conglomerate wherein only foldamer molecules adopting a right-handed helical screw-sense preference (*i.e.*, *P*-helicity) are present.[47] The helical pitch of the foldamer found in the crystal structure of **1**·butanone is 3.4 Å, which is comparable to that observed in **1**·THF.

In an analogous manner to **1**·THF, the butanone-containing solvatomorph of **1** exhibits a crystal packing arrangement wherein columnar stacks are composed of foldamer molecules adopting only one helical screw sense (*e.g.*, only *P*-helicity). Furthermore, as with **1**·THF, butanone solvent molecules reside within the void spaces of the channel aggregates that are formed within this structure. These channels have a diameter of 9.0 Å and the observed increase in dimensions compared to **1**·THF (*cf.* 7.8 Å for **1**·THF *vs.* 9.0 Å for **1**·butanone, see Table 1) is likely a consequence of the differing sizes, shapes and/or orientations of the THF and butanone solvent molecules within the channels. Unlike in **1**·THF, there is no disorder about the solvent molecules in **1**·butanone so it is possible to identify the relative head-to-tail orientation of the solvent molecules within the channel cavities (see Fig. 5a). The presence of the butanone solvent molecules within the channels of **1**·butanone is stabilised by the formation of an intermolecular hydrogen-bonding interaction between the foldamer and solvent molecules for the majority component. Hence, as in **1**·THF, there is an intermolecular N–H⋯O hydrogen-bonding interaction involving the NH atom of one of the terminal amine functionalities of the foldamer and the O atom of the solvent molecule which stabilises the observed crystal packing arrangement (see Fig. 5b).[49]

Crystallographic analysis of 1·DCM. Single crystals of **1**·DCM were grown through the slow vapour diffusion of diethyl ether into a saturated dichloromethane solution of **1** (see Fig. 6). In the unit cell of **1**·DCM, there are two foldamer molecules (one *M*-helicity and one *P*-helicity) which shows that this solvatomorph is a racemate in the solid state. In **1**·DCM, there is also one dichloromethane solvent molecule. The foldamer molecules in **1**·DCM adopt a tight helical conformation with a pitch value of 3.3 Å, which is similar to that seen for **1**·THF and **1**·butanone (*cf.* 3.3 Å for **1**·DCM, *cf.* 3.4 Å for **1**·THF and **1**·butanone). In an analogous manner to **1A** and **1B**, the crystal packing arrangement of **1**·DCM adopts columnar stacks of molecules composed of alternating helices with opposite screw-sense preferences. This is distinct from **1**·THF and **1**·butanone for which only one helical screw-sense preference (*e.g.*, *P*-helicity) is observed and is a consequence of the fact that **1**·THF and **1**·butanone form conglomerates and **1A**, **1B** and **1**·DCM are racemates (see Table 1). As with **1**·THF and **1**·butanone, the dichloromethane solvatomorph **1**·DCM adopts a crystal packing arrangement wherein solvent molecules are present within the cavities of the channels in the structure. Unlike in **1**·THF and **1**·butanone, in **1**·DCM, the dichloromethane solvent molecules adopt an arrangement wherein each foldamer molecule lies in close proximity to six solvent molecules that are arranged to give a six-fold order of symmetry within the system (see Fig. 6a). The dimensions of the
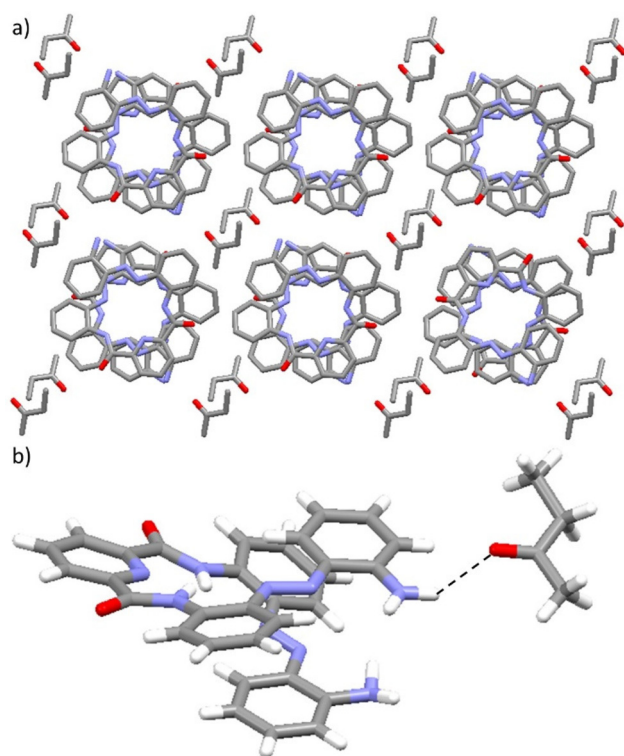
5594 | *Org. Biomol. Chem.*, 2025, **23**, 5590–5599

This journal is © The Royal Society of Chemistry 2025

Fig. 6 X-ray structure of **1**·DCM: (a) viewed along the *c*-axis highlighting the presence of the dichloromethane solvent molecules within the void spaces of the crystal packing arrangement of the structure; (b) showing the presence of intermolecular N−H⋯Cl and aliphatic C−H⋯O hydrogen-bonding interactions between the foldamer and the dichloromethane solvent molecules which help stabilise their incorporation into the channel cavities within the structure. C atoms are shown in grey, O in red, N in light blue, Cl in light green and H in white. H-bonding interactions are shown as dashed red lines. H atoms have been removed from (a) for clarity.

Fig. 7 X-ray structure of **1**·MeOH: (a) highlighting the presence of the methanol solvent molecules within the void spaces of the crystal packing arrangement of the structure; (b) showing the presence of intermolecular N−H⋯O and O−H⋯O hydrogen-bonding interactions between the foldamer and the methanol solvent molecules which stabilise their incorporation into the channel cavities within the structure. C atoms are shown in grey, O in red, N in light blue and H in white. H-bonding interactions are shown as dashed red lines. H atoms have been removed from (a) for clarity.
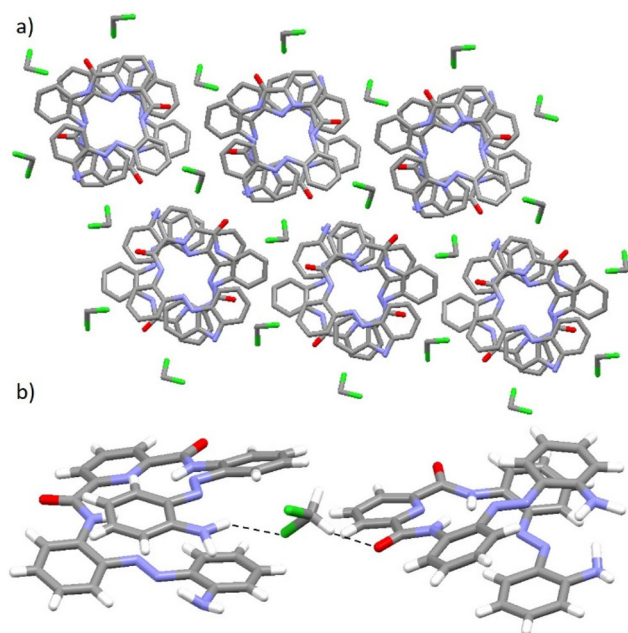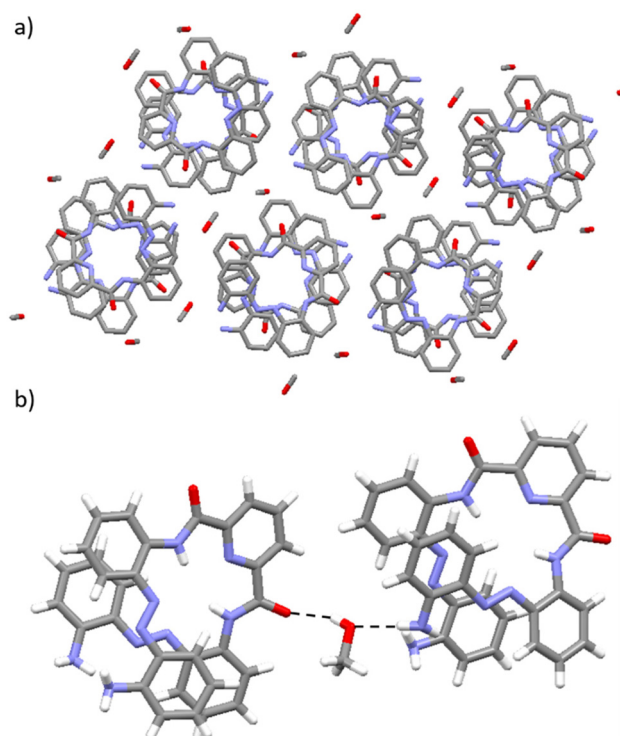
channels within **1**·DCM have diameters of 4.3 Å which is significantly smaller than those observed in **1**·THF and **1**·butanone of 7.8 Å and 9.0 Å respectively (see Table 1). Presumably, the crystal packing arrangement of the molecules within the cavity is considerably influenced by the size, shape and/or orientation of the solvent molecules as well as their ability to form non-covalent interactions with the foldamer that stabilise their encapsulation within the cavities of the structure.

The crystal packing arrangement of **1**·DCM is stabilised by the presence of two types of intermolecular hydrogen bonding interactions formed between one dichloromethane solvent molecule and two foldamers of opposite helical screw-sense preferences in adjacent columnar stacks (see Fig. 6b). First, an intermolecular N−H⋯Cl hydrogen-bonding interaction[50] is observed between an NH on a terminal amine group of a foldamer molecule and the Cl atom of a dichloromethane solvent molecule. Second, an aliphatic C−H⋯O interaction[51] is present between an H atom on the same dichloromethane solvent molecule and an O atom of the carbonyl bond in a second foldamer molecule in a neighbouring columnar stack.

Crystallographic analysis of 1·MeOH. Slow evaporation of a saturated methanol/dichloromethane solution of **1** yielded crystals of **1**·MeOH which were of sufficiently good quality for single-crystal X-ray diffraction analysis (see Fig. 7). In the unit cell of **1**·MeOH, there are two distinct foldamer molecules (one with

M-helicity and one with *P*-helicity) and two methanol solvent molecules, showing that **1**·MeOH is a racemate in the solid state.

In the crystal packing arrangement of **1**·MeOH, columnar stacks composed of *M*- and *P*-helical foldamers are observed, which is in line with the structures exhibited by the other identified racemates of **1A**, **1B** and **1**·DCM. **1**·MeOH forms cavities within the solid state with a diameter of 3.5 Å (see Table 1). These cavities are considerably smaller than those observed for **1**·THF and **1**·butanone of 7.8 Å and 9.0 Å respectively and slightly smaller than those observed in **1**·DCM of 4.3 Å. In an analogous manner to **1**·THF, **1**·butanone, **1**·CH$_2$Cl$_2$ and **1**·DMSO, the solvent molecules in **1**·MeOH are encapsulated within the channel cavities of the structure. However, it is likely that the differing sizes, shapes and/or orientations of the distinct solvent molecules within these solvatomorphs (of **1**·THF, **1**·butanone, **1**·CH$_2$Cl$_2$ and **1**·MeOH) and their varying ability to form a range of non-covalent interactions with the foldamer molecule, to stabilise their encapsulation, strongly influence the dimensions of the channels and cavities adopted within the solid state.

As with **1**·DCM, the methanol-containing solvatomorph exhibits a crystal packing arrangement where each foldamer

This journal is © The Royal Society of Chemistry 2025

Org. Biomol. Chem., 2025, **23**, 5590–5599 | **5595**

molecule is oriented closely to six solvent molecules (see Fig. 7a). The crystal packing arrangement in **1**·MeOH is stabilised through two distinct types of hydrogen-bonding interactions formed between the methanol solvent molecule and the foldamer. First, intermolecular N–H···O hydrogen-bonding interactions are present between an amine functionality at the termini of the foldamer and the O atom within the methanol solvent molecule (see Fig. 7b). Second, intermolecular O–H···O hydrogen-bonding interactions are formed between the hydroxyl group of a methanol solvent molecule and the O atom of the carbonyl group in the foldamer (see Fig. 7b).[49]

Crystallographic analysis of 1·DMSO. From a DMSO solution of **1** at ambient temperature, single crystals suitable for X-ray diffraction analysis of **1**·DMSO were obtained (see Fig. 8). **1**·DMSO forms a conglomerate in the solid state, wherein only foldamer molecules of one type of helicity (*M*-helicity) are present.[47] There is also one DMSO solvent molecule present in

the unit cell of **1**·DMSO which exhibits disorder about all the atoms in the solvent molecule (see the ESI†). There is also disorder about a terminal aromatic ring and the corresponding amine functionality for the foldamer molecule in the unit cell of **1**·DMSO (see the ESI†). The **1**·DMSO solvatomorph exhibits a helical pitch value of 3.3 Å, indicating the presence of a tightly wound and compact helical structure in the solid state (*cf.* 3.3 Å for **1**·DCM, *cf.* 3.4 Å for **1**·THF, **1**·butanone and **1A**-*I*).

The crystal packing arrangement observed in **1**·DMSO involves the adoption of columnar stacks of foldamer molecules exhibiting only *M*-helicity (see Fig. 8a). This is in contrast to the other studied solvatomorphs of the foldamer which exhibit columnar stacks of alternating *M*- and *P*-helical foldamers as they are racemates (*e.g.*, **1A**, **1B** and **1**·DCM). In an analogous manner to **1**·THF and **1**·butanone, solvent molecules are incorporated into the cavities of the channels formed within the columnar stack crystal packing arrangement of **1**·DMSO. Furthermore, MoloVol[42] analysis of **1**·DMSO shows that this structure exhibits a channel packing arrangement with a diameter of 8.7 Å (see Table 1). This is considerably larger than those observed in **1**·DCM and **1**·MeOH but slightly larger than those seen in **1**·THF (*cf.* 7.8 Å for **1**·THF *vs.* 8.7 Å for **1**·DMSO, see Table 1). The varying diameters of the identified channels in the different solvatomorphs are likely due to varying sizes and shapes of the solvent molecules that are incorporated within the channels and/or their relative orientations within the supramolecular channel aggregates.

The presence of the DMSO solvent molecules within **1**·DMSO is stabilised by intermolecular C–H···O hydrogen-bonding interactions that are formed between the aliphatic protons of the DMSO solvent molecule and the O atom of an adjacent DMSO solvent molecule (see Fig. 8b). These intermolecular non-covalent interactions formed between DMSO solvent molecules lead to the formation of a one-dimensional C–H···O hydrogen-bonded chain in the solid state wherein the DMSO solvent molecules adopt a head-to-tail geometry within the structure. No intermolecular hydrogen-bonding interactions are observed which involve the amine functionality in the foldamer and solvent molecule. Instead, the NH atoms in the terminal amine functionalities of the foldamers of **1**·DMSO form an intermolecular N–H···O hydrogen-bonding interaction with the O atom of the amide bond in the central carboxamide moiety of an adjacent foldamer molecule (see the ESI†).

Fig. 8 X-ray structure of **1**·DMSO: (a) viewed along the *b*-axis highlighting the presence of the DMSO solvent molecules within the void spaces of the crystal packing arrangement of the structure; (b) showing the presence of intermolecular C–H···O hydrogen-bonding interactions between DMSO solvent molecules, which form the basis of a one-dimensional hydrogen-bonding chain. C atoms are shown in grey, O in red, N in light blue, S atoms in yellow and H in white. H-bonding interactions are shown as dashed red lines. H atoms have been removed from (a) for clarity. The disorder about the DMSO solvent molecules and the aromatic ring and amine functionality of the foldamer have been removed for clarity.

Conclusions

The solvatomorphism of a diamine-terminated 2,6-pyridyldicarboxamide-based foldamer **1** has been investigated in a range of solvents through the solid-state analysis of a range of solvatomorphs including **1A**, **1B**, **1**·DCM, **1**·THF, **1**·butanone, **1**·MeOH and **1**·DMSO. Single-crystal X-ray diffraction analysis has been used to establish the influence of the nature of the solvent on the conformational behaviour and crystal packing arrangements adopted in these supramolecular systems. **1A**,
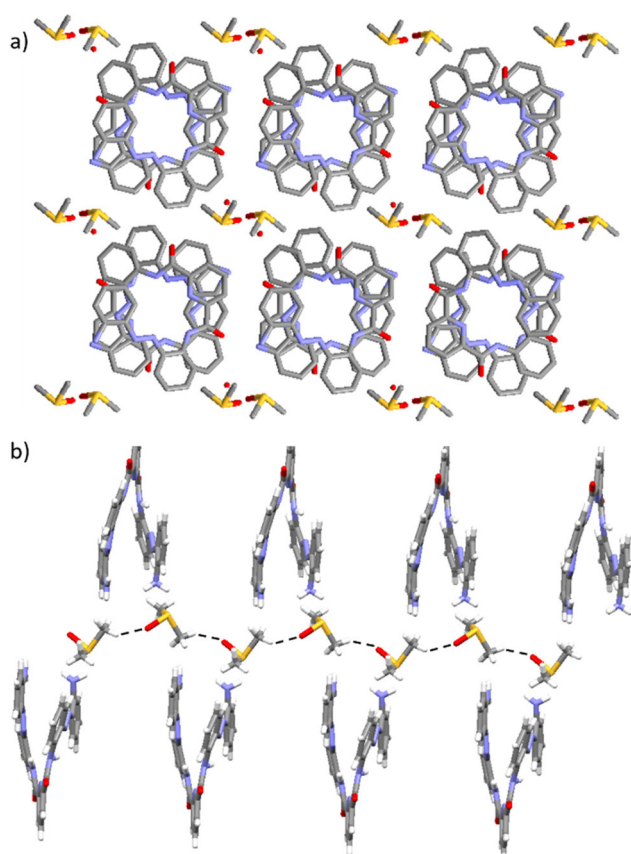
5596 | *Org. Biomol. Chem.*, 2025, **23**, 5590–5599

This journal is © The Royal Society of Chemistry 2025

1B, 1·DCM and 1·MeOH have been shown to exist as racemates in the solid state whilst 1·THF, 1·butanone and 1·DMSO form conglomerates. These conglomerates could be a useful source of enantio-enriched solid foldamers in the future.[47]

All of the studied solvatomorphs, of 1A, 1B, 1·DCM, 1·THF, 1·butanone, 1·MeOH and 1·DMSO, adopt a stable helical conformation, which establishes that the nature of the solvent does not perturb the secondary structure of these supramolecular scaffolds in the solid state. Notably, the solvent-free solvatomorphs of 1 (*i.e.*, 1A, 1B) do not exhibit channels whilst those incorporating solvents into the solid-state structure (*i.e.*, 1·DCM, 1·THF, 1·butanone, 1·MeOH and 1·DMSO) adopt supramolecular aggregates of channels. Additionally, in the case of 1·DMSO, a solvent-based one-dimensional hydrogen-bonded chain is observed.

Crystallographic analysis shows that the dimensions of the channels found in 1·DCM, 1·THF, 1·butanone, 1·MeOH and 1·DMSO vary significantly in diameter between 3.5 and 9.0 Å. These observed variations in the cavity sizes within the crystal packing arrangements of the studied solvatomorphs of 1, 1·DCM, 1·THF, 1·butanone, 1·MeOH and 1·DMSO are likely due to their ability to encapsulate the appropriate solvents, which have differing sizes, shapes and orientations, within the channel cavities (*i.e.*, dichloromethane for 1·DCM, tetrahydrofuran for 1·THF, butanone for 1·butanone, methanol for 1·MeOH and dimethylsulfoxide for 1·DMSO). Finally, it has been established that the incorporation of the different solvents into the channel cavities of the distinct solvatomorphs of the studied foldamers is stabilised by the presence of a diverse array of intermolecular hydrogen-bonding interactions, including N–H⋯O, N–H⋯Cl, O–H⋯O, N–H⋯Cl and C–H⋯O, formed between the foldamer and/or solvent molecule(s).

Given the relevance of systematic solid-state studies in improving our understanding of the fundamental features that govern the conformational behaviour of foldamers and the underexplored role of solvatomorphism in these supramolecular scaffolds, we anticipate that this work will help enable the future design of new foldamers and optimise the performance of existing ones. This is particularly relevant to the emerging solid-state applications of foldamers (*e.g.*, in crystal engineering) as well as their potential long-term applications (*e.g.*, in biological chemistry). Additionally, supramolecular scaffolds that can form solvent-mediated 1D networks are the subject of great interest due to their potential applications in the uptake and storage of small molecules for potential uses in energy and materials chemistry.

Data availability

The data supporting this article including crystallisation screening conditions and crystallographic analysis have been included as part of the ESI.† Crystallographic data for 1A, 1B, 1·THF, 1·butanone, 1·MeOH and 1·DMSO have been deposited at the CCDC and can be found in CIF and other electronic formats with the following CCDC numbering; 1A: 2426430,

1A′: 2426870, 1B: 2426871, 1·THF: 2426432, 1·butanone: 2426872, 1·DCM: 2426428, 1·MeOH: 2426873, 1·DMSO: 2426874.

Conflicts of interest

There are no conflicts to declare.

Acknowledgements

References

1 (*a*) H. Juwarker, J.-M. Suk and K.-S. Jeong, *Chem. Soc. Rev.*, 2009, **38**, 3316–3325; (*b*) D.-W. Zhang, X. Zhao, J.-L. Hou and Z. T. Li, *Chem. Rev.*, 2012, **112**, 5271–5316.

2 (*a*) D. J. Hill, M. J. Mio, R. B. Prince, T. S. Hughes and J. S. Moore, *Chem. Rev.*, 2001, **101**, 3893; (*b*) I. Saraogi and A. D. Hamilton, *Chem. Soc. Rev.*, 2009, **38**, 1726; (*c*) T. A. Martinek and F. Fülöp, *Chem. Soc. Rev.*, 2012, **41**, 687.

3 (*a*) G. Guichard and I. Huc, *Chem. Commun.*, 2011, **47**, 5933; (*b*) B. A. F. Le Bailley and J. Clayden, *Chem. Commun.*, 2016, **52**, 4852.

4 (*a*) Z. C. Girvin and S. H. Gellmann, *J. Am. Chem. Soc.*, 2020, **142**, 17211; (*b*) D. Bécart, V. Diemer, A. Salaün, M. Oiarbide, Y. R. Nelli, B. Kauffmann, L. Fishcer, C. Palomo and G. Guichard, *J. Am. Chem. Soc.*, 2017, **139**, 12524; (*c*) C. Ma, J. Tang, L. Yu, K. Wen and Q. Gan, *Chem. – Eur. J.*, 2022, **28**, e202200834.

5 Q. Lin, C. Ma, R. T. Stendall, K. Shankland, R. A. Musgrave, P. N. Horton, C. Baldauf, H.-J. Hofmann, C. P. Butts, M. M. Müller and A. J. A. Cobb, *Angew. Chem., Int. Ed.*, 2023, **62**, e202305326.

6 H. Juwarker and K.-S. Jeong, *Chem. Soc. Rev.*, 2010, **39**, 3664.

7 (*a*) D.-W. Zhang, X. Zhao and Z.-T. Li, *Acc. Chem. Res.*, 2014, **47**, 1961; (*b*) J. Shen, C. Ren and H. Zeng, *J. Am. Chem. Soc.*, 2017, **139**, 3587.

8 (*a*) Y. Zhao and Z. Zeng, *J. Am. Chem. Soc.*, 2006, **128**, 9988; (*b*) H. Li, L. Liang, B. Ku, W. Zhao, X.-J. Yang and B. Wu, *Chem. Sci.*, 2022, **13**, 4915.

This journal is © The Royal Society of Chemistry 2025

Org. Biomol. Chem., 2025, **23**, 5590–5599 | **5597**

9 (*a*) M. Pasco, C. Dolain and G. Guichard, *Comprehensive Supramolecular Chemistry II*, Elsevier, 2017, p. 89; (*b*) D. Deepak, J. Wu, V. Corvaglia, L. Allmendinger, M. Schechenbach, P. Tinnefeld and I. Huc, *Angew. Chem., Int. Ed.*, 2024, e202422958.

10 (*a*) A. D. Peters, S. Borsley, F. della Sala, D. F. Cairns-Gibson, M. Leonidou, J. Clayden, G. F. S. Whitehead, I. J. Vitórica-Yrezábal, E. Takano, J. Burthem, S. L. Cockroft and S. J. Webb, *Chem. Sci.*, 2020, **11**, 7023; (*b*) R. Gopalakrishnan, A. I. Frolov, L. Knerr, W. J. Drury III and E. Valeur, *J. Med. Chem.*, 2016, **59**, 9599.

11 (*a*) G. W. Collie, K. Pulka-Ziach and G. Guichard, *Chem. Sci.*, 2016, **7**, 3377; (*b*) V. Pavone, S.-Q. Zhang, A. Merlino, A. Lombardi, Y. Wu and W. F. DeGrado, *Nat. Commun.*, 2014, **5**, 3581; (*c*) L. A. Estroff, C. D. Incarvito and A. D. Hamilton, *J. Am. Chem. Soc.*, 2003, **126**, 2; (*d*) X. Hu, S. J. Dawson, P. K. Madal, X. de Hatten, B. Baptiste and I. Huc, *Chem. Sci.*, 2017, **8**, 3741.

12 (*a*) J. Solà, M. Bolte and I. Alfonso, *CrystEngComm*, 2016, **18**, 3793; (*b*) C. Tomasini, N. Castellucci, V. C. Caputo, L. Milli, G. Battistelli, S. Fermani and G. Falini, *CrystEngComm*, 2014, **17**, 116; (*c*) C. Dutta, P. Krishnamurthy, D. Su, S. H. Yoo, G. W. Collie, M. Pasco, J. K. Marzinek, P. J. Bond, C. Verma, A. Gréland, A. Loquet, J. Li, M. Luo, M. Barboiu, G. Guichard, R. M. Kini and P. P. Kumar, *Chem*, 2023, **9**, 2237.

13 C. Dutta, P. Krushnamurthy, D. Su, S. H. Yoo, G. W. Collie, M. Pasco, J. K. Marzinek, P. J. Bond, C. Verma, A. Grélard, A. Loquet, J. Li, M. Luo, M. Barboiu, G. Guichard, R. M. Kini and P. P. Kumar, *Chem*, 2023, **9**, 2237.

14 F. Qin, M. Sheng, R. Li, D. Liu, M. Ren, R. Tian, L. Douadji, D. Wang, Q. Gan and L. Liang, *Chem. Eng. J.*, 2024, **489**, 151006.

15 H. G. Brittain, *J. Pharm. Sci.*, 2012, **101**, 464.

16 M.-I. Delegkou, N. Panagiotou, C. Papatriantafyllopoulou, A. Tasipoulos, D. Papaioannou, S. P. Perlepes and V. Nastopoulos, *CrystEngComm*, 2024, **26**, 3574.

17 (*a*) S. J. Pike, A. D. Bond and C. A. Hunter, *CrystEngComm*, 2018, **20**, 2912; (*b*) P. Panini, E. Boel, L. Van Meerpikvelt and G. Van den Mooter, *Cryst. Growth Des.*, 2022, **22**, 2703; (*c*) H. Lemmer, N. Steiger, W. Liebenberg and M. R. Caira, *Cryst. Growth Des.*, 2012, **12**, 1683.

18 M. Jurić, B. Perić, N. Brničević, P. Planinić, D. Pajić, K. Zadro, G. Giester and B. Kaitner, *Dalton Trans.*, 2008, 842.

19 A. Suhonen, E. Nauha, K. Salorinne, K. Helttunen and M. Nissinen, *CrystEngComm*, 2012, **14**, 7398.

20 T. Qi, V. Maurizot, H. Noguchi, T. Charoenraks, B. Kauffmann, M. Takafuji, H. Ihara and I. Huc, *Chem. Commun.*, 2012, **48**, 6337.

21 M. T. Stone, J. M. Fox and J. S. Moore, *Org. Lett.*, 2004, **6**, 3317.

22 B. A. F. Le Bailly, L. Byrne, V. Diemer, M. Foroozandeh, G. A. Morris and J. Clayden, *Chem. Sci.*, 2015, **6**, 2313.

23 (*a*) F. Meng, X. Zhang, T. Sarma, N. Yuan, Y. Yin, Z. Duan, C. Lei, Q. Qian, L. Ding and Z. Zhang, *CrystEngComm*, 2019, **21**, 3906; (*b*) A. A. Nalawade, N. G. Kumar, K. R. P. Kumar, M. Singh, S. Dey and H. N. Gopi, *CrystEngComm*, 2024, **26**, 913.

24 (*a*) F. S. Menke, B. Wicher, L. Allmendinger, V. Maurizot and I. Huc, *Chem. Sci.*, 2023, **14**, 3742; (*b*) A. Meunier, M. L. Singleton, B. Kauffmann, T. Granier, G. Lautrette, Y. Ferrand and I. Huc, *Chem. Sci.*, 2020, **11**, 12178; (*c*) K. Urushibara, Y. Ferrand, Z. Liu, K. Katagirim, M. Kawahata, E. Morvan, R. D'Elia, V. Pophristic, A. Tanatani and I. Huc, *Chem. – Eur. J.*, 2021, **27**, 11205.

25 (*a*) S. J. Pike, J. E. Jones, J. Raftery, J. Clayden and S. J. Webb, *Org. Biomol. Chem.*, 2015, **13**, 9580; (*b*) S. J. Pike, T. Boddaert, J. Raftery, S. J. Webb and J. Clayden, *New J. Chem.*, 2015, **39**, 3288; (*c*) S. J. Pike, J. Raftery, S. J. Webb and J. Clayden, *Org. Biomol. Chem.*, 2014, **12**, 4124.

26 (*a*) F. S. Menke, B. Wicher, V. Maurizot and I. Huc, *Angew. Chem., Int. Ed.*, 2023, **62**, e202217325; (*b*) A. Borissov, I. Marques, J. Y. C. Lim, V. Félix, M. D. Smith and P. D. Beer, *J. Am. Chem. Soc.*, 2019, **141**, 4119; (*c*) S. J. Pike, V. Diemer, J. Raftery, S. J. Webb and J. Clayden, *Chem. – Eur. J.*, 2014, **20**, 15981; (*d*) C.-Z. Liu, S. Koppireddi, H. Wang, D.-W. Zhang and Z.-T. Li, *Angew. Chem., Int. Ed.*, 2018, **58**, 226.

27 (*a*) W. Cai, G.-T. Wang, Y.-X. Xu, X.-K. Jiang and Z.-T. Li, *J. Am. Chem. Soc.*, 2008, **130**, 6936; (*b*) L.-Y. You, G. T. Wang, X.-K. Jiang and Z. T. Li, *Tetrahedron*, 2009, **65**, 9494.

28 C.-Z. Liu, C. Zhang, C.-G. Li, H. B. Chen, W. Yang, Z.-Y. Li, Z.-Y. Hu, L. Xu, B. Zhai and Z.-T. Li, *Chem. – Eur. J.*, 2024, **30**, e202401150.

29 F. S. Menke, B. Wicher, V. Maurixot and I. Huc, *Angew. Chem., Int. Ed.*, 2023, **62**, e202217325.

30 R. A. Dodson, A. P. Kalenak and A. J. Matzger, *J. Am. Chem. Soc.*, 2020, **142**, 20806.

31 H. Yang, H. Zhang, C. J. Kang, C. Ji, D. Shi and D. Zhao, *Sci. Adv.*, 2024, **10**, eads0260.

32 A. A. Jones and C. D. Snow, *Chem. Commun.*, 2024, **60**, 5790.

33 D. R. Brown, M. J. Hurlock, T. M. Nenoff and J. M. Rimsza, *ACS Appl. Mater. Interfaces*, 2025, **17**, 5496.

34 A. Suhonen, M. Kortelainen, E. Nauha, S. Yliniemelä-Sipari, P. M. Pihko and M. Nissinen, *CrystEngComm*, 2016, **18**, 2005.

35 R. Annala, A. Suhonen, H. Laakkonen, P. Permi and M. Nissinen, *Chem. – Eur. J.*, 2017, **23**, 16671.

36 A. Suhonen, M. Kortelainen, E. Nauha, S. Yliniemelä-Sipari, P. M. Pihko and M. Nissinen, *CrystEngComm*, 2016, **18**, 2005.

37 R. Annala, A. Suhonen, H. Laakkonen, P. Permi and M. Nissinen, *Chem. – Eur. J.*, 2017, **23**, 16671.

38 (*a*) A. R. Davis, S. Ozturk, C. C. Seaton, L. Male and S. J. Pike, *Chem. – Eur. J.*, 2024, **30**, e202402892; (*b*) A. R. Davis, J. O. Dismorr, J. H. R. Tucker and S. J. Pike, *Chem. – Eur. J.*, 2024, **30**, e202402423.

39 S. J. Pike, R. Telford and L. Male, *Org. Biomol. Chem.*, 2023, **21**, 7717.

5598 | *Org. Biomol. Chem.*, 2025, **23**, 5590–5599

This journal is © The Royal Society of Chemistry 2025

40 S. J. Pike, A. Heliot and C. C. Seaton, *CrystEngComm*, 2020, **40**, 4030.

41 In this foldamer class, we have previously defined the helical pitch value as the distance between the C atoms present in terminal amide functionalities, see: A. R. Davis, S. Ozturk, C. C. Seaton, L. Male and S. J. Pike, *Chem. – Eur. J.*, 2024, **30**, e202402892 for more detailed examples. However, the lack of terminal amine groups in **1** means that we have calculated the helical pitch values as the distance between the N atoms of the terminal amine functionalities in this study. See ESI† for further details.

42 J. B. Maglic and R. Lavendomme, *J. Appl. Crystallogr.*, 2022, **55**, 1033.

43 (*a*) C. A. Hunter, *Angew. Chem., Int. Ed.*, 2004, **43**, 5310; (*b*) C. A. Hunter, J. Singh and J. M. Thornton, *J. Mol. Biol.*, 1991, **218**, 837.

44 I. Rozas, I. Alkorta and J. Elguero, *J. Phys. Chem. A*, 1998, **102**, 9925–9932.

45 Y. Hamuro, S. J. Geib and A. D. Hamilton, *J. Am. Chem. Soc.*, 1997, **119**, 10587.

46 Short contacts between the N atoms of the azo bonds and the H atom of the adjacent amine group are observed in all solid state structures of **1** and these could serve to further stabilise the helical structure of the scaffold. Similar short contacts have been reported by Parquette and co-workers in their related pyridinedicarboxamide/*m*-(phenylazo)azobenzene foldamers, see: C. Tie, J. C. Gallucci and J. R. Parquette, *J. Am. Chem. Soc.*, 2006, **128**, 1162.

47 M. P. Walsh, J. A. Barclay, C. S. Begg, J. Xuan and M. O. Kitching, *Cryst. Growth Des.*, 2023, **23**, 2837.

48 H. J. Shen, R. Ye, A. Romanies, A. Roy, F. Chen, C. Ren, Z. Liu and H. Zeng, *J. Am. Chem. Soc.*, 2020, **142**, 10050.

49 J. Shen, R. Ye, A. Romanies, A. Roy, F. Chen, C. Ren, Z. Liu and H. Zeng, *J. Am. Chem. Soc.*, 2020, **142**, 10050.

50 E. P. Aldrich, K. A. Bussey, J. R. Connell, E. F. Reinhart, K. D. Oshin, B. Q. Mercado and A. G. Oliver, *Acta Crystallogr., Sect. E: Crystallogr. Commun.*, 2016, **72**, 40–43.

51 S. Horowitz and R. C. Trievel, *J. Biol. Chem.*, 2012, **287**, 41576.

This journal is © The Royal Society of Chemistry 2025

Org. Biomol. Chem., 2025, **23**, 5590–5599 | **5599**